Energy-Transfer Upconversion and Thermal Lensing in High-Power End-Pumped Nd : YLF Laser Crystals

P. J. Hardman, W. A. Clarkson, G. J. Friel, M. Pollnau, and D. C. Hanna

***Abstract*— Thermal lensing in an end-pumped Nd : YLF rod, under lasing and nonlasing conditions, has been investigated. Under lasing conditions, a weak thermal lens, with dioptric power varying linearly with pump power, was observed. Under nonlasing conditions, where higher inversion densities were involved, hence relevant to Q-switched operation or operation as an amplifier, a much stronger thermal lens was measured, whose power increased nonlinearly with pump power. This difference has been attributed to the increased heat deposition due to the subsequent multiphonon decay following various interionic upconversion processes, which increase strongly under nonlasing conditions, and is further exacerbated by the unfavorable temperature dependencies of heat conductivity and the rate of change of the refractive index with temperature. A strategy for reducing upconversion and its associated thermal loading, without degrading laser performance, is discussed.**

***Index Terms*— Diode-pumped lasers, laser amplifiers, lasers, laser thermal factors, neodymium:solid-state lasers, upconversion.**

I. Introduction

POWER-SCALING of diode-end-pumped solid-state lasers to multiwatt output power, while retaining the high efficiency and diffraction-limited beam quality that have been characteristic of operation at low powers, is attracting growing attention [1], [2] due to the numerous potential applications of such sources. However, progress has been hindered by two main problems. Firstly, the highly elliptical nature of the output beams from high-power diode bars, and, secondly, the onset of strong thermal effects which result from the high thermal loading density in end-pumped lasers. With the introduction of effective beam-shaping schemes [3], enabling the equalization of beam quality factors in orthogonal planes and hence focusing to high-intensity beams, thermal effects have become the major limitation. Generation of heat in the laser medium is a fundamental problem which ultimately sets limits on the maximum operating power. For many laser transitions, the energy difference (quantum defect) between pump photon and laser photon energy establishes a minimum heat input. Thus, in a Nd : YLF system, operating at a wavelength of 1053 nm, pumped by a diode laser operating at 797 nm, the quantum defect implies that the minimum amount of heat produced is $\sim$24% of the absorbed pump energy. Removal of this heat requires a nonuniform temperature distribution within the laser medium and, consequently, leads to a thermally induced lensing behavior. Three processes contribute to this thermal lens: a change in the refractive index with temperature, stress-induced changes in the refractive index, and bulging of the end faces via differential expansion.

One attractive feature of Nd : YLF, which was recognized early in its development [4], [5], is its weaker thermal lens compared to Nd : YAG for the same pumping conditions. This is a consequence of YLF showing a decrease of refractive index with increasing temperature, creating a negative thermal lens, which is partly offset by the positive lens due to the bulging of the rod end faces. The degree of compensation of these opposite contributions to thermal lensing is particularly evident for the σ-polarization (corresponding to 1.053-μm operation), where the net thermal lensing is $\sim$17 times weaker than for a comparable 1.064-μm Nd : YAG laser [6]. Other advantages of Nd : YLF include its natural birefringence and its long fluorescence lifetime. The latter feature is of interest for high-power Q-switched operation. In practice, however, it has been noted that it is difficult, with end-pumped lasers, to realize this supposed benefit for Q-switching, and recent research [7], [8] indicates that possible reasons are to be found in the detrimental effect of energy-transfer upconversion (ETU). ETU is a process in which one excited ion, in the $^4F_{3/2}$ upper laser level, relaxes down to a lower lying level and transfers its energy to a neighboring excited ion, also in the $^4F_{3/2}$ level, which is thereby raised (upconverted) to a higher level. Hence, ETU reduces the population of the upper laser level, effectively shortening its lifetime.

Thermal lensing is a critical factor for resonator design and must be thoroughly understood and characterized if an optimum design for efficient operation is to be achieved. In this paper, we describe the measurement of thermal lensing in end-pumped Nd : YLF crystals under lasing and nonlasing conditions. Both sets of measurements were taken, since as well as designing CW lasers we wished to extend the design to Q-switched lasers, for which the excitation density for low repetition-rate Q-switching is close to that under nonlasing conditions. These measurements are described in Section II. A significant difference in thermal lens power between lasing and nonlasing conditions was observed, with a much stronger lens power under nonlasing conditions. This we attribute to ETU. Thus, besides the decreased performance under Q-switched operation, noted above, it also leads to

Manuscript received July 20, 1998; revised December 7, 1998. This work was supported by the Engineering and Physical Sciences Research Council. The work of P. J. Hardman was supported by Lumonics, Ltd., through a Cooperative Award in Science and Engineering Studentship. The work of M. Pollnau was supported by the European Union within the "Human Capital and Mobility Programme" through a fellowship.

The authors are with the Optoelectronics Research Centre, University of Southampton, Southampton SO17 1BJ, U.K.

Publisher Item Identifier S 0018-9197(99)02532-4.

additional heat generation, via subsequent multiphonon decay, and hence stronger thermal lensing. A simple analytical model has been developed to test this explanation and is described in Section III. The full analysis is confined to the appendix. With this better understanding of the thermal lensing behavior in diode-pumped Nd : YLF, it appears that this material now has very good prospects for further power scaling in spite of it having a low fracture limit, which is ~5 times lower than that for Nd : YAG. Using the appropriate design strategy, it should be possible to scale diode-end-pumped Nd : YLF lasers with TEM_{00} output to powers well in excess of 10 W.

II. Experimental

Several different techniques have been used for measuring thermally induced lensing in laser media [6], [9], [10]–[12], and measurements of thermal lensing behavior in Nd : YLF have been previously made [5], [6], [9], [10], [12], [13]. However, most of the work has been carried out on lamp-pumped lasers, involving a more or less uniform heat deposition, whereas, by contrast, end-pumped lasers typically experience an essentially Gaussian transverse heat deposition. In addition, a direct comparison between lensing behavior for lasing and nonlasing conditions for varying pump power has not yet been reported in the literature. In this section, we describe the measurement of thermal lensing under lasing and nonlasing conditions within a Nd : YLF system end-pumped by a diode bar.

In our measurements, the pump characteristics were kept the same under both lasing and nonlasing conditions. The pump was provided by a 20-W diode bar whose output beam was reconfigured by a two-mirror beam shaper, described in detail in [3]. Application of this beam shaper has allowed effective pumping for various lasers [14], [15]. In this experiment, the focusing optics were configured to produce a beam of waist radii 340 μm×220 μm with corresponding M^2 values of 79 and 63. The rod was oriented with its c axis parallel to the resonator plane, and, in order to reduce the risk of thermally induced fracture, the diode wavelength was temperature detuned from the absorption peak, at ~797 nm, to longer wavelengths until an absorption length of ~3 mm was obtained in the Nd : YLF. The 6-mm-long × 4-mm-diameter Nd : YLF rod (1.15 at% doping) was mounted in a water-cooled copper heat sink, which provided side-cooling of the rod. The temperature of the cooling water was held at 288 K. The pump was always operated at maximum power and attenuated by using a half-wave plate and polarizing beam splitter to allow the pump power to be varied without altering the pump geometry inside the rod.

Nd : YLF is a uniaxial birefringent crystal with significant anisotropy in a number of its properties, in particular exhibiting a change in refractive index with temperature (dn/dT) of -4.3×10^{-6} K^{-1} for π-polarization ($\boldsymbol{E}$-field vector parallel to the c axis) and -2.0×10^{-6} K^{-1} for σ-polarization ($\boldsymbol{E}$-field vector perpendicular to the c axis) [4], [6]. Thus, to fully characterize the thermal lens, four measurements need to be taken, i.e., for lensing in the two orthogonal planes of the crystal and for both π- and σ-polarizations.

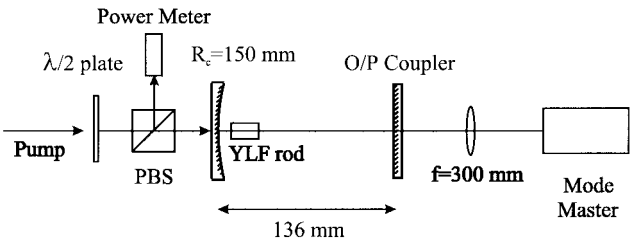

Fig. 1. Experimental setup used for measuring the power of the thermal lens under lasing conditions.

Measurements of the thermal lens under lasing conditions were initially made. The basic procedure involved constructing a simple end-pumped laser resonator with a plane output coupler and measuring the TEM_{00} mode waist size on the plane output coupler. With a knowledge of the resonator parameters, except for the thermal lens focal length, it was possible to calculate the latter through the ABCD matrix formalism for Gaussian beams. Thus, the cavity needed to be kept simple to allow accurate modeling and chosen to have a large change in spot size on the output coupler for change in thermal lens so as to increase the sensitivity of the measurement. The cavity design chosen (Fig. 1) was a simple two-mirror resonator, close to half-confocal, with a 150-mm radius-of-curvature mirror and a plane output coupler $(R = 90\%)$, separated by 136 mm and the Nd : YLF rod placed 10 mm away from the curved mirror. The laser typically had a threshold of ~700 mW and an output power of ~2.7 W for ~8.5 W of incident pump power. The output from the laser was collimated by a lens of focal length $f_1 = 300$ mm, positioned ~300 mm from the output coupler, and was then incident on a Coherent Modemaster. The latter was used to measure the M^2 beam propagation factor and the collimated waist size w_2 after lens f_1. The waist radius w_1 on the output coupler could then be simply calculated from

$$w_1 = \frac{M^2 f_1 \lambda}{\pi w_2}. \tag{1}$$

The accuracy of this technique was limited by the uncertainty in the measurement of the cavity length (estimated to be ±1 mm) and by the uncertainty in the focal length of the collimating lens (stated by the manufacturer to be ±2%). The combined effect of these uncertainties resulted in a systematic error for the calculated values of thermal lens focal length versus pump power typically within the range ±30%.

The thermal lens was also measured under nonlasing conditions, in which there is a much larger population in the upper laser level, corresponding to typical conditions of low-repetition-rate Q-switching. Under these conditions, the Nd : YLF is more susceptible to processes such as energy-transfer upconversion [7], [8] involving closely neighboring ions both in the upper laser level. Since we were primarily concerned with obtaining focal length values for the thermal lens and less interested in any spherical aberration of the lens, a probe-beam technique was used in which the probe beam size was chosen to be significantly smaller than the pump beam size (in this case, approximately half the pump beam size), thus sampling the maximum on-axis value of

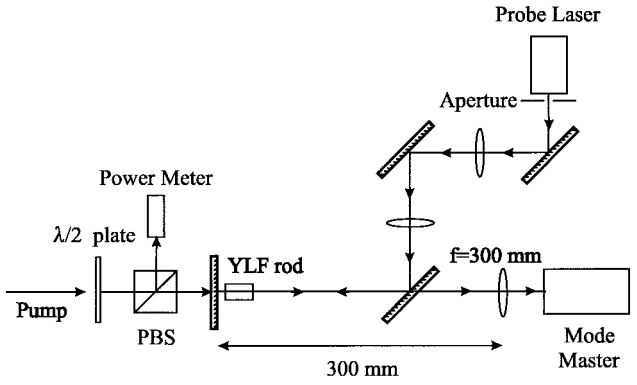

Fig. 2. Experimental setup used for measuring the power of the thermal lens under nonlasing conditions.

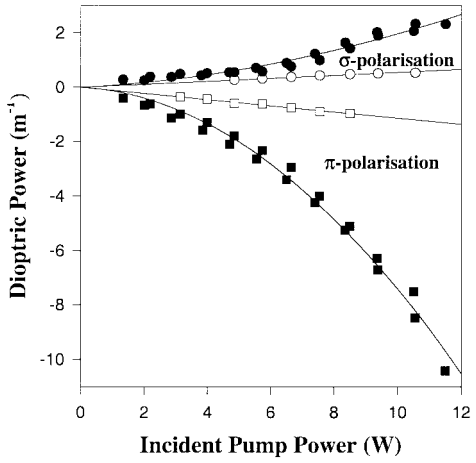

Fig. 3. Measurements of thermal lens power, for both polarizations (squares for π-polarization, circles for σ-polarization), under lasing (open symbols) and nonlasing (solid symbols) conditions for the direction perpendicular to the c axis.

the thermal lens. The probe beam was provided by a diode-pumped Nd : YAG laser operating at 1064 nm, as shown in Fig. 2. The linearly polarized output of the Nd : YAG laser was collimated by a lens of focal length 250 mm and focused by a lens of focal length 200 mm to produce a beam waist of 150-μm radius close to the pump input face of the Nd : YLF rod. The probe light was then reflected to pass through the Nd : YLF rod for a second time by a highly reflecting mirror positioned at the probe beam waist. The high reflector was tilted slightly away from normal incidence to avoid feeding back the probe light to the Nd : YAG probe laser. Finally, the probe beam was focused by a lens of focal length $f = 300$ mm located at a distance equal to its focal length (i.e., 300 mm) from the pump input face of the Nd : YLF rod, and the waist location was determined with a Coherent Modemaster. Using the ABCD matrix formalism, a relationship can be derived between the waist distance x from the final focusing lens and the focal length $f_{\rm th}$ of the thermal lens. If the separation of the Nd : YLF rod and high reflector is much shorter than both $f_{\rm th}$ and the Rayleigh range (as was the case in our experimental arrangement), then the expression for $f_{\rm th}$ simplifies to

$$f_{\rm th} = \frac{-2f^2}{\Delta x} \tag{2}$$

where Δx is the difference between final waist positions with and without the thermal lens. Thus, by measuring Δx, the thermal lens can easily be determined. A half-wave plate was added to the setup when the orthogonal polarization was required. The probe beam was carefully aligned along the pump axis, using two steering mirrors, to obtain good overlap. The alignment was aided by blocking the pump and then observing how the probe was displaced when the pump was unblocked. A perfectly aligned beam was simply expanded but undisplaced. The final alignment was carried out quantitatively by measuring the thermal lens and adjusting the probe position until the strongest thermal lens was obtained. The accuracy of this technique was limited by the uncertainty in the focal length of the lens and the uncertainty of the measurement of the waist location (stated to be $\pm(8\%|Z_0| + 4$ cm), where Z_0 is the distance from the front bezel plane reference on the ModeMaster Scan Head to the beam waist. The combined effect of these uncertainties resulted in a systematic error typically within the range $\pm$30%. This was confirmed by replacing the rod by lenses of known focal length.

Fig. 3 gives the results of measuring the thermal lens under both lasing and nonlasing conditions. Dioptric power of the lens is plotted against incident pump power. Only results for the direction perpendicular to the c axis are given because, in the direction parallel to the c axis, the lens was too weak for accurate measurement. This is believed to be due to the elliptical pump beam profile which was larger in the c direction, thus reducing the corresponding lens power. The results under lasing conditions are indicated as open symbols. These results show a linear variation of dioptric power of the thermal lens with incident pump power, as would be expected from a model which ignores ETU [6], [16]. For the π-polarization (corresponding to lasing at 1047 nm), the thermally induced lens is negative. This is due to the strong negative contribution from dn/dT, dominating the positive contribution from the bulging of the end faces. However, for the σ-polarization (corresponding to lasing at 1053 nm), which has a smaller negative dn/dT, it is the lens created by the bulging of the end faces which dominates and overall leads to a positive lens. For both polarizations, the overall lens is of weaker power, compared to that observed in Nd : YAG under similar pump conditions [17].

The results under nonlasing conditions are given by the solid symbols. Each polarization demonstrates the same sign of lens under lasing and nonlasing conditions. However, there are two significant differences between the lens observed under lasing and nonlasing conditions. Under nonlasing conditions, the lens is significantly stronger and has a nonlinear variation with pump power. At the maximum pump power of 12 W incident on the crystal, the dioptric power measured under nonlasing conditions is a factor $\sim$6 times larger than the value measured for lasing conditions, for both the σ- and π-polarizations. However, this measured difference in the thermal lensing for nonlasing and lasing conditions is slightly exaggerated since different experimental conditions were used for the different measurement techniques. Under nonlasing

conditions, the probe beam had a spot radius of 150 μm, whereas under lasing conditions the spot radius was 300 μm. Since the pump beam has a "Gaussian-like" intensity profile, the thermal lens is highly aberrated and can be thought of as a lens whose focal length varies radially, decreasing in strength (dioptric power) as radial separation r from the center of the pumped region increases. Thus, both of our techniques for measuring the thermal lens focal length (dioptric power) yield average values which depend on the probe beam/laser mode size. For a pump beam with a Gaussian intensity profile, it can be shown, by simply calculating a weighted average dioptric power over the probe beam/laser mode sizes, that the net result is that the ratio of the dioptric powers measured under nonlasing and lasing conditions is exaggerated by a factor of ~1.2. Thus, in reality, the ratio of the dioptric powers at the maximum available pump power is ~5. Since this large difference was at first considered surprising, a second set of measurements was taken, giving similar results, as shown in Fig. 3 by the pairs of points at the various pump powers. Also, as a further experimental check, we compared directly the thermal lens under lasing and nonlasing conditions using a single-pass He–Ne beam to probe the thermal lens. By viewing the alteration of the beam size after passing through the rod, we were again able to confirm directly the large difference in the thermal lensing between lasing and nonlasing conditions.

III. Analysis and Discussion

We have developed an approximate analytical model of the thermal lensing behavior to provide a quantitative guide to the expected lensing power. For simplicity, the model considers only contributions to thermal lensing arising from the temperature dependence of the refractive index. In Nd : YLF, other contributions to thermal lensing, most notably end-face curvature, make a significant contribution to the net thermal lens. This is particularly so on the 1053-nm transition (σ-polarization) and less so on the 1047-nm transition (π-polarization) for which dn/dT is greater. However, assuming that the contribution of end-face bulge to the thermal lens has the same pump power dependence as the lensing due to dn/dT [18], one can then compare the relative strength of thermal lensing under lasing and nonlasing conditions by considering just that part of the lensing which arises from dn/dT. All measurements were taken with fixed pump size, fixed absorption length, and fixed output mirror transmission (hence fixed threshold), so that the relative contribution of the end-face curvature and internal lensing remained fixed.

To determine the dioptric power of thermally induced lensing, we must first identify the dominant processes which create heat in the crystal. Fig. 4 shows the energy-level scheme of Nd : YLF with all the major processes identified.

A. Thermal Lensing Without Upconversion

We first consider the situation without upconversion. Pump radiation is absorbed from the ground state ($^4I_{9/2}$) to the pump level ($^4F_{5/2}$) from where it relaxes, via multiphonon emission, to the upper laser level, thereby generating heat. Heat is also generated via the mutiphonon decay to the ground state after each of the four fluorescence processes, shown in Fig. 4. The dashed lines in Fig. 4 indicate the relevant heat generating processes. Under lasing conditions, significant heat is generated only by multiphonon decay from the pump band to the upper laser level ($^4F_{5/2} \rightarrow {}^4F_{3/2}$) and from the lower laser level to the ground state ($^4I_{11/2} \rightarrow {}^4I_{9/2}$). Hence, the fraction ρ_L of the absorbed pump converted to heat is ~24%. However, under nonlasing conditions, the upper laser level decays via all the four fluorescent processes, i.e., emitting at 1830 nm ($^4F_{3/2} \rightarrow {}^4I_{15/2}$), at 1330 nm ($^4F_{3/2} \rightarrow {}^4I_{13/2}$), at 1050 nm ($^4F_{3/2} \rightarrow {}^4I_{11/2}$), at 900 nm and ($^4F_{3/2} \rightarrow {}^4I_{9/2}$), as well as via multiphonon decay on the transition $^4F_{3/2} \rightarrow {}^4I_{15/2}$. This gives the respective branching ratios $\beta_{43} = 0.04$ (86% of which is due to nonradiative decay), $\beta_{42} = 0.115, \beta_{41} = 0.523$, and $\beta_{40} = 0.322$ [19]. Hence, under nonlasing conditions, the fraction ρ_{nL} of the absorbed pump converted to heat is ~25%. The dioptric power is approximately proportional to the fractional heating. Thus, if the effect of upconversion is neglected, the induced thermal lens, for nonlasing conditions, would be only $\rho_{nL}/\rho_L \sim 1.05$ times stronger than for lasing conditions. This small additional heat loading under nonlasing conditions does not account for the increases in the thermal lens observed in the experiment.

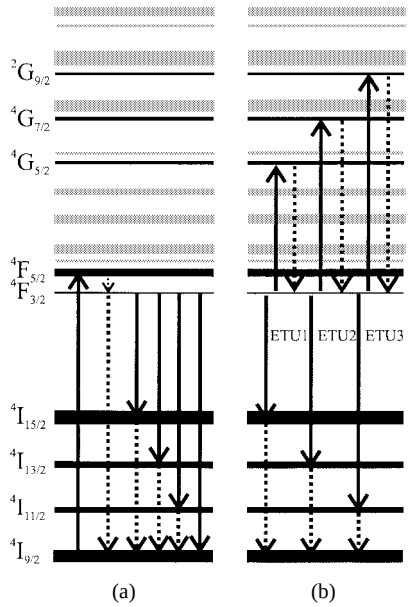

Fig. 4. Energy-level scheme of Nd : YLF. All dashed lines indicate heat generating processes. (a) Without ETU. (b) With ETU.

B. Thermal Lensing with Upconversion

To explain the observed difference in thermal lensing under lasing and nonlasing conditions, we must also take account of the effect of upconversion. ETU is a process in which one excited ion, in the $^4F_{3/2}$ upper laser level, relaxes down to a lower lying level and transfers the corresponding energy to a neighboring excited ion which is upconverted to an upper level. There are three dominant upconversion mechanisms [19] shown in Fig. 4 as ETU1–ETU3. In ETU1, relaxation of an ion in the upper laser level ($^4F_{3/2}$) to the lower level $^4I_{15/2}$ results in an excitation of a neighboring ion in the

upper laser level to the $^4G_{5/2}$ level. Similarly, in ETU2, relaxation to the lower level $^4I_{13/2}$ results in an excitation to the $^4G_{7/2}$ level, and in ETU3 relaxation down to the lower level $^4I_{11/2}$ results in an excitation to the $^4G_{9/2}$ level. These three processes have a direct spectral overlap and hence do not themselves create heat. However, heat is generated through the subsequent multiphonon relaxation from the excited level back to the upper laser level and from the lower level down to the ground state, as shown in Fig. 4 by the dashed lines. All three ETU processes emit the same heat which is equivalent to a complete nonradiative relaxation of one ion from the upper laser level down to the ground state (i.e., 92% of the energy of an absorbed pump photon). Thus, the relative contributions to thermal loading under nonlasing conditions, including the effect of upconversion, can be deduced as follows. Multiphonon relaxation from the pump level to the upper laser level converts 0.08 of the absorbed pump to heat. For the fraction γ of excited Nd^{3+} ions in the upper-laser level which decay via the fluorescence processes, the contribution to thermal loading is 0.17γ of the absorbed pump power. The remaining $(1-\gamma)$ Nd^{3+} ions contribute to thermal loading via one of the three ETU processes, resulting in a fractional heating of $0.92(1-\gamma)$. Hence for a pump beam with a Gaussian intensity profile

$$I_p(r,z) = \frac{2P_p}{\pi w_p^2}\ \exp\left(-\frac{2r^2}{w_p^2} - \alpha_p z\right) \tag{3}$$

the net thermal loading density $Q(r,z)$ under nonlasing conditions can be expressed in the form

$$\begin{aligned} Q(r,z) = &[0.08 + 0.17\gamma(r,z) \\ &+ 0.92(1-\gamma(r,z))]\alpha_p I_p(r,z) \end{aligned} \tag{4}$$

where P_p is the incident pump power, w_p is the $1/e^2$ beam radius, and α_p is the absorption coefficient for the pump. We have assumed here, as appropriate for the Nd^{3+} ion, that the pumping quantum efficiency is 1, i.e., each pump photon produces a Nd^{3+} ion in the $^4F_{3/2}$ state.

Equation (4) can be generalized for both lasing and nonlasing conditions by

$$Q(r,z) = [1-(1-\rho)\gamma(r,z)]\alpha_p I_p(r,z) \tag{5}$$

where ρ is the fraction of the absorbed pump converted to heat in the absence of upconversion. Thus, if upconversion dominates (i.e., $\gamma \to 0$), then all the pump power could be converted to heat, and, if there was no upconversion (i.e., $\gamma \to 1$), then the fraction ρ of the pump power is converted to heat.

One can calculate γ by using a simple rate-equation approach. Since the decay rate, via multiphonon processes, is fast compared to the fluorescence lifetime τ, it can be shown [8], [19] that the combined effect of the different upconversion processes can be expressed by a single rate parameter $W = 1.7 \times 10^{-16}$ cm^3/s and, finally, that the net effect is the removal of only one excitation from $^4F_{3/2}$ by each upconversion process, since the upconverted ion will decay rapidly back to the upper laser level. Thus, one obtains

$$\frac{dN}{dt} = R - \frac{N}{\tau} - WN^2 \tag{6}$$

where R is the pumping rate per unit volume ($R \equiv (R(r,z) = \alpha_p I_p(r,z)/h\nu_p)$) and N is the upper laser level population.

Then, from (6), one obtains the following expression for steady-state inversion density:

$$N_s = \frac{-\tau^{-1} + (\tau^{-2} + 4WR)^{1/2}}{2W}. \tag{7}$$

Hence, the fraction $\gamma(r,z)$ of excited Nd^{3+} ions which decay via the fluorescence processes is given by

$$\gamma(r,z) = \frac{-\tau^{-1} + (\tau^{-2} + 4WR(r,z))^{1/2}}{2W\tau R(r,z)}. \tag{8}$$

Thus, by substituting (8) into (5), one can determine the effect of ETU on the thermal loading density. Clearly, the effect of upconversion will be most pronounced at the center of the pumped region $(r=0)$ where the pump rate is largest. Equation (8), for $\gamma(r,z)$, is only strictly valid under nonlasing conditions. However, an approximate value for $\gamma(r,z)$ and hence the thermal loading density, under lasing conditions, can be obtained by replacing $R(r,z)$ in (8) by the threshold pump rate density, since, under lasing conditions, $R(r,z)$ would be clamped at the threshold value.

With a knowledge of thermal loading density $Q(r,z)$, we can now derive an expression for the thermal lens dioptric power, at the center of the pumped region $(r=0)$, taking into account the influence of ETU. To simplify the analysis, we have assumed that the rod is side-cooled with heat flowing only radially from the pumped region and that the pump beam radius is approximately constant over the Nd:YLF crystal length. We have also assumed that the rod is long enough so that all of the pump is absorbed and that there is no ground state bleaching. The details of this derivation are described in the appendix; here, we merely quote the resulting expression for dioptric power D, namely

$$\begin{aligned} D = D_{\max}\Bigg\{1 - \frac{2(1-\rho)}{\beta}\ \Bigg[2(\sqrt{1+\beta}-1) \\ +\ \ln\left(\frac{4}{\beta}\ \frac{\sqrt{1+\beta}-1}{\sqrt{1+\beta}+1}\right)\Bigg]\Bigg\} \end{aligned} \tag{9}$$

where β is a measure of the magnitude of the effect of upconversion on the overall decay rate from the upper laser level, β being proportional to the pump power absorbed per unit volume and the upconversion rate W. β is given by

$$\beta = \frac{8WP_p\alpha_p\tau^2}{\pi w_p^2 h\nu_p} \tag{10}$$

and $D_{\max}$ is the maximum dioptric power under operating conditions where upconversion is very strong (i.e., $\beta \to \infty$), so that all of the absorbed pump is converted to heat. If we consider only the contribution to thermal lensing which arises from the temperature dependence of the refractive index, then $D_{\max}$ is given by the approximate expression

$$D_{\max} = \frac{P_p dn/dT}{\pi w_p^2 K_c} \tag{11}$$

where K_c is the thermal conductivity and dn/dT is the change in refractive index with temperature.

The contribution to thermal lensing by end-face bulge is assumed to have the same dependence on absorbed power as the internal (dn/dT) lensing, thus the net lensing power should have essentially the same dependence on the degree of ETU as observed by the right-hand side of (9). It can be seen from (9) that, when $\beta \to 0$ (i.e., the effect of upconversion is negligible), then $D \to D_{\max}\rho$ as expected. The value for β defined in (10) applies to nonlasing conditions. Under CW lasing conditions, the inversion density and hence ETU rates are clamped at the threshold value. Hence, the dioptric power under lasing conditions $D_{\rm las}$ is given by the modified expression

$$D_{\rm las} = D_{\rm th} + \frac{(P_p - P_{p\rm th})\rho\, dn/dT}{\pi w_p^2 K_c} \tag{12}$$

where $P_{p\rm th}$ is the threshold pump power and $D_{\rm th}$ is the dioptric power at threshold, given by (9) with $P_p = P_{p\rm th}$. Hence, under CW lasing conditions, the influence of upconversion is generally much smaller than under nonlasing conditions.

The following parameters used in our experiment, described in Section II, are substituted into (9) for the π-polarization and perpendicular to the c axis: $\tau = 520\ \mu$s, $\alpha_p = 333\ \text{m}^{-1}$, $\lambda_p = 797$ nm, $dn/dT = -4.3 \times 10^{-6}\ \text{K}^{-1}$, $W = 17 \times 10^{-23}\ \text{m}^3 \cdot \text{s}^{-1}$, $K_c = 6.25\ \text{W}\cdot\text{m}^{-1}\ \text{K}^{-1}$ (at 288 K), and $w_p = 235\ \mu$m (which is the average spot size weighted to the absorption distribution). Then, evaluating the dioptric powers for nonlasing and lasing conditions, we can calculate that the effect of the extra heat generated as a result of upconversion is to increase the dioptric power under nonlasing conditions by a factor of $\sim$2.7 (from lasing conditions) at the maximum pump power of $\sim$12 W incident on the Nd : YLF rod. Under lasing conditions, we estimate that the influence of upconversion is to increase the strength of thermal lensing by a factor of $\sim$1.03 compared to the situation without upconversion. However, it should be noted that, if an output coupler of higher transmission is used, hence increasing the threshold, then upconversion may become an important consideration.

The calculated ratio ($\sim$2.7) of dioptric powers under nonlasing and lasing conditions due to the influence of upconversion is significant but still does not fully account for our experimental measurements, which suggest a ratio of dioptric powers of $\sim$5. However, a further increase in dioptric power arises from the fact that the thermal conductivity and dn/dT are themselves temperature-dependent, particularly under nonlasing conditions. Thus, the elevated temperature in the pumped region results in a decrease in thermal conductivity and an increase in $|dn/dT|$. The temperature dependence of thermal conductivity [6] is approximately given by

$$K(T) = K_0 \cdot \frac{T_0}{T} \tag{13}$$

where T is the absolute temperature and K_0 is the thermal conductivity at a characteristic temperature T_0. For Nd : YLF, $K_0 = 6\ \text{W}\cdot\text{m}^{-1}\ \text{K}^{-1}$ at $T_0 = 300$ K.

We have estimated the additional contribution to thermal lensing due to the decrease in thermal conductivity with temperature, using an approximate numerical model to calculate the average temperature along the axis of the Nd : YLF rod at the center of the pumped region. At the maximum pump power, the average temperature, over an absorption length, was calculated to be $\sim$337 K under lasing conditions and $\sim$434 K under nonlasing conditions at a heat sink temperature of 288 K. This results in thermal conductivities under lasing and nonlasing conditions of 5.3 and 4.1 $\text{m}^{-1} \cdot \text{K}^{-1}$, respectively. This leads to a further increase in the ratio of the thermal lens powers to $\sim$3.5.

This result still remains smaller than the ratio of lens powers measured experimentally, although within experimental uncertainties, which were rather large for the measurement techniques used, as explained in Section II. This approximate model still excludes contributions to lensing which may arise due to the variation with temperature of dn/dT and of the expansion coefficient. Also, the model does not include the stronger absorption in the wings of the diode spectrum (the diode was offset from the absorption peak), which will increase the upconversion at the front end of the rod. The model also assumes an average temperature distribution throughout the rod, whereas, in fact, the change in thermal conductivity will be more marked at the front of the rod. Incorporating all of these effects into the model would lead to a further increase in the predicted ratio of dioptric power under nonlasing and lasing conditions. Regardless of these details, this approximate analytical model clearly demonstrates the important role of ETU and its associated multiphonon relaxation in generating additional heat in Nd : YLF under typical end-pumping conditions, leading to a marked increase in thermal lens power, particularly at the high inversion densities present under nonlasing conditions.

C. Strategy for Reducing Upconversion

In general, it would be advantageous to reduce the influence of upconversion without significantly reducing the overall laser efficiency. This is particularly important for Q-switched lasers or high-gain amplifiers, where the increase in thermal lens power density due to ETU would, for example, make stable resonator designs more difficult to realize and would probably lead to a degradation in laser beam quality due to the highly aberrated nature of the lens. From (9), we obtain the following expression for the ratio of thermal lens powers with and without ETU, under nonlasing conditions:

$$\Gamma_{\rm upcon} = \frac{1}{\rho}\left\{1 - \frac{2(1-\rho)}{\beta}\left[2(\sqrt{1+\beta}-1) + \ln\left(\frac{4}{\beta}\left(\frac{\sqrt{1+\beta}-1}{\sqrt{1+\beta}+1}\right)\right)\right]\right\}. \tag{14}$$

The above expression can be used as a guide to the magnitude of the effect of ETU and hence develop a strategy for reducing its influence. This equation can be used for other laser transitions in Nd : YLF or, indeed, for other Nd-doped materials with similar upconversion processes, provided that the corresponding upconversion parameter W is known. Fig. 5 shows the variation of $\Gamma_{\rm upcon}$ with the dimensionless parameter β. From Fig. 5, it can be seen that in order to render the effect of ETU on thermal lensing negligible it is necessary to design the laser system so that β is very small.

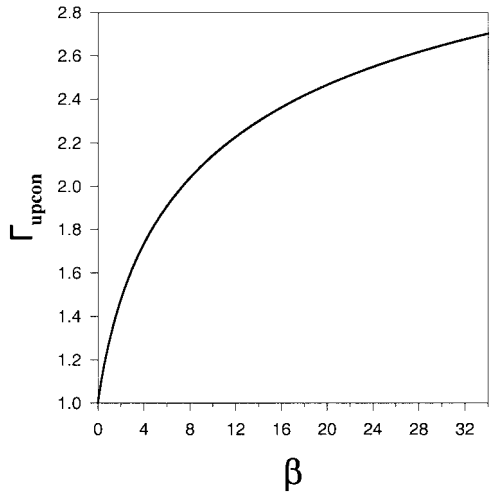

Fig. 5. The dimensionless parameter $\Gamma_{\rm upcon}$ against β for $\rho = 0.25$.

For example, to ensure that the increase in dioptric power due to ETU is less than 30%, then the upper limit on β is $\sim$1.3. However, it should be noted that (14) only applies to the center of the pumped region, and, since ETU is smaller in the wings of the pumped region, this upper limit can be somewhat increased. For four-level laser operation at $\sim$1 μm, a reduction in β can be achieved without compromising laser efficiency by decreasing W (by decreasing the dopant concentration and thus decreasing energy migration within the upper laser level). In Nd:YAG, the upconversion parameter W varies linearly with Nd concentration [20], and we would tentatively assume a similar relationship in Nd:YLF. Alternatively, β can be reduced by decreasing the absorption coefficient (by detuning the temperature of the diode or decreasing the dopant concentration). Clearly, adopting these measures requires a pump beam with adequate beam quality so that there is little diffraction spreading of the pump beam over the longer length of the laser rod required for efficient pump absorption.

For the conditions used in the experiment, described in Section II, we obtain a β value of $\sim$34 (giving a $\Gamma_{\rm upcon}$ of $\sim$2.7) under nonlasing conditions. Obviously, a low-repetition-rate Q-switched laser system based on the design described in Section II would clearly suffer from a reduced gain and increased thermal lensing due to ETU. However, by incorporating the measures outlined above, it should be possible to design a Q-switched laser system that avoids the detrimental influence of upconversion.

IV. Summary

We have characterized the thermal lensing in a diode-bar end-pumped Nd:YLF laser rod under lasing and nonlasing conditions. Under lasing conditions, a weak thermal lens, which varied linearly with pump power, was observed. Under nonlasing conditions, a much stronger thermal lens was measured, the power of which increased nonlinearly with pump power. At maximum incident pump power, a difference of a factor of $\sim$5 in thermal lens power between lasing and nonlasing conditions was observed. This difference has been explained by the additional heat generated via multiphonon relaxation following ETU processes. The strength of the thermal lensing is further compounded by the unfavorable temperature dependence of crystal properties such as heat conductivity and dn/dT. The result is that, at some pump power level, there is a rather rapid onset of steeply worsening thermal effects as pump power is further increased. In turn, the increase in thermal lens power can give rise to a rather pronounced deterioration in laser performance at high pump intensities, and careful design is needed to avoid such problems if successful scaling up of Nd:YLF performance is to be achieved, whether in CW, Q-switched, or amplifier schemes. A simple analytical model for thermal lensing which takes into account the influence of ETU has been presented, and a strategy for power scaling by reducing its effect has been discussed. With the appropriate precautions (e.g., reduction of dopant concentration) to reduce the role of ETU, further power scaling should indeed be possible without compromising laser efficiency or beam quality.

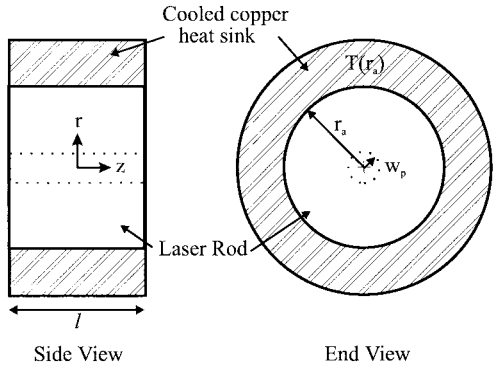

Fig. 6. Heat sink mounting for an edge-cooled rod of radius r_a and length l.

Appendix A
Thermal Lensing Without Upconversion

We consider a side-cooled rod of radius r_a and length l mounted as shown in Fig. 6 and end-pumped by a diode laser with incident power $\boldsymbol{P}_p$. The heat flux $h(r,z)$ under steady-state conditions must satisfy the general equation

$$\nabla \cdot \boldsymbol{h}(r,z) = Q(r,z) \tag{A1}$$

where $Q(r,z)$ is the power per unit volume deposited as heat in the laser medium. The heat flux is related to the corresponding temperature distribution within the crystal by

$$\boldsymbol{h}(r,z) = -K_c \nabla \boldsymbol{T}(r,z) \tag{A2}$$

where K_c is the thermal conductivity of the laser material.

If we now assume that heat flow is radial with the temperature at the rod edge equal to the heat-sink temperature $T(r_a)$, then, from (A1), we can deduce the net radial heat flow from a thin disc of radius r and thickness Δz at axial position z by [16]

$$2\pi r \Delta z h(r,z) = \int_z^{z+\Delta z} \int_0^r Q(r',z') 2\pi r' \, dr' \, dz' \tag{A3}$$

where $\boldsymbol{h}(r,z)$ is now the radial heat flux.

If we make the simplifying assumptions that the ground state is not significantly depleted and that the pump beam has a Gaussian intensity profile with pump beam radius w_p which does not vary significantly over the length of the pumped region in the rod, then $Q(r,z)$ can be written as

$$Q(r,z) = \rho\alpha_p I_p(r,z) \tag{A4}$$

where

$$I_p(r,z) = \frac{2P_p}{\pi w_p^2}\ \exp\left[\frac{-2r^2}{w_p^2} - \alpha_p z\right] \tag{A5}$$

is the pump intensity, ρ is the fraction of absorbed pump power converted to heat, w_p is the $1/e^2$ radius of the pump beam, α_p is the absorption coefficient, and P_p is the incident pump power.

Thus, by substituting (A4) into (A3), we can obtain an expression for the radial heat flux $\boldsymbol{h}(r,z)$

$$h(r,z) = \frac{\alpha_p \rho P_p}{2\pi} \cdot \exp(-\alpha_p z)\left(\frac{1-\exp(-2r^2/w_p^2)}{r}\right). \tag{A6}$$

The distribution of temperature difference ΔT inside the crystal $(\Delta T(r,z) \equiv T(r,z) - T(r_a,z))$ can be calculated by substituting (A6) into (A2), i.e.,

$$\Delta T(r,z) = \frac{1}{K_c}\int_r^{r_o} h(r,z)\,dr. \tag{A7}$$

The resulting radial variation in optical path difference (OPD) created by this temperature distribution can be calculated using

$$\mathrm{OPD}(r) = \frac{dn}{dT}\int_0^l \Delta T(r,z)\,dz \tag{A8}$$

where dn/dT is the change in refractive index with temperature.

Now, for a thin thermal lens, with a given radially varying OPD, an approximate expression for the thermal lens power $D(r)$ can be derived from simple geometrical considerations

$$D(r) = \frac{1}{f_t(r)} = \frac{l\,\dfrac{dn(r)}{dr}}{r} = \frac{\dfrac{d\,\mathrm{OPD}(r)}{dr}}{r}. \tag{A9}$$

From (A9), it can be seen that if $\mathrm{OPD}(r) \propto r^2$, then the dioptric power is independent of r, i.e., the lens has no phase aberration and hence will not degrade the beam quality.

Thus, an expression for the distributed thermal lens can be written as

$$D(r) = \frac{dn/dT}{K_c}\,\frac{\rho P_p}{2\pi}\,\frac{(1-\exp(-\alpha_p l))\left(1-\exp\left(\dfrac{-2r^2}{w_p^2}\right)\right)}{r^2}. \tag{A10}$$

If we assume that the rod is long compared to the absorption length so that $1-\exp(-\alpha_p \cdot l) \sim 1$, then the thermal lens power at the center of the pumped region $(r=0)$ is given by

$$D(0) = \frac{dn/dT}{K_c}\,\frac{\rho P_p}{\pi w_p^2}. \tag{A11}$$

Appendix B
Thermal Lensing with Upconversion

If we restrict our considerations to the center of the pumped region where the thermal lens is strongest, then the pump intensity becomes

$$I_p(z) = \frac{2P_p}{\pi w_p^2}\ \exp(-\alpha_p z). \tag{A12}$$

Including the additional heat generated due to ETU, the power per unit volume deposited as heat $Q(z)$ can be written as

$$Q(z) = \alpha_p I_p(z)[1-(1-\rho)\gamma(z)] \tag{A13}$$

where ρ is the fraction of absorbed pump power converted to heat without upconversion and γ is the fraction of excited Nd^{3+} ions in the upper laser level which decay via the fluorescence processes.

We can calculate γ by using a simple rate-equation approach. Since decay via the multiphonon processes is fast compared with τ, the combined effect of the different upconversion processes can be expressed by a single parameter W, and the effect is for only one excitation to be removed from the ${}^4F_{3/2}$ level by each upconversion process, since the upconverted ion will decay rapidly to the upper laser level. Thus, we obtain

$$\frac{dN}{dt} = R - \tau^{-1}N - WN^2 \tag{A14}$$

where $R(z)$ is the pumping rate per unit volume $(=\alpha_p I_p(z)/h\nu_p)$, τ is the fluorescence lifetime, and N is the upper laser level population.

From (A14), we obtain the following expression for steady-state inversion density:

$$N_s = \frac{-\tau^{-1} + (\tau^{-2} + 4WR)^{1/2}}{2W}. \tag{A15}$$

Hence, the fraction of excited ions which decay by fluorescence processes is given by

$$\gamma(z) = \frac{-\tau^{-1} + (\tau^{-2} + 4WR(z))^{1/2}}{2W\tau R(z)}. \tag{A16}$$

So, substituting (A16) into (A13) gives

$$Q(z) = \alpha_p I_p(z) - \frac{(1-\rho)hc}{2W\tau\lambda_p}\left(-\frac{1}{\tau} + \sqrt{\frac{1}{\tau^2} + 4WR(z)}\right). \tag{A17}$$

By substituting (A17) into (A3), we can obtain an expression for the radial heat flux and, substituting this into (A7)–(A9),

we obtain an equation for dioptric power of the thermal lens at the center of the rod

$$D_{\mathrm{ETL}}(0) = \frac{1}{K_c}\frac{dn}{dT}\left[\frac{P_p}{\pi w_p^2}\left(1-e^{-\alpha_p l}\right) - \frac{(1-\rho)h\nu_p}{4W\tau} \cdot \int_0^l \left(-\frac{1}{\tau}+\sqrt{\frac{1}{\tau^2}+4WR(z)}\right)dz\right]. \tag{A18}$$

Now

$$\begin{aligned}\int_0^l &\left(-\frac{1}{\tau}+\sqrt{\frac{1}{\tau^2}+4WR(z)}\right)dz \\ &= -\frac{l}{\tau} - \frac{2}{\alpha_p\tau}\left[1+\beta e^{-\alpha_p l}\right]^{1/2} + \frac{2}{\alpha_p\tau}\left[1+\beta\right]^{1/2} \\ &\quad + \frac{2}{\alpha_p\tau}\operatorname{arctanh}\left[(1+\beta e^{-\alpha_p l})^{1/2}\right] \\ &\quad - \frac{2}{\alpha_p\tau}\operatorname{arctanh}[(1+\beta)^{1/2}]\end{aligned} \tag{A19}$$

where β is a dimensionless parameter, which provides a measure of the contribution from the ETU processes and is given by

$$\beta = \frac{8WP_p\alpha_p\tau^2}{\pi w_p^2 h\nu_p}. \tag{A20}$$

Expression (A20) applies for nonlasing conditions; for lasing conditions, where the inversion density is clamped, the pump power P_p should be replaced by the threshold pump power.

Expression (A18) for D_{ETU} can be simplified if it is assumed that all the pump is absorbed, i.e., the rod is long compared to the absorption coefficient. So, with this assumption, the final expression for dioptric power is given by

$$D_{\mathrm{ETU}}(0) = \frac{P_p\, dn/dT}{\pi w_p^2 K_c}\left\{1-\frac{2(1-\rho)}{\beta}\left[2(\sqrt{1+\beta}-1) + \ln\left(\frac{4}{\beta}\left(\frac{\sqrt{1+\beta}-1}{\sqrt{1+\beta}+1}\right)\right)\right]\right\}. \tag{A21}$$

REFERENCES

[1] W. L. Nighan, D. Dudley, and M. S. Keirstead, "Diode-bar-pumped Nd:YVO_4 lasers with >13-W TEM_{00} output at >50% efficiency," in *Conf. Lasers and Electro-Optics OSA Tech. Dig. Ser.*, 1995, vol. 15, p. 17.

[2] W. A. Clarkson, P. J. Hardman, and D. C. Hanna, "High-power diode-bar end-pumped Nd:YLF laser at 1.053 μm," *Opt. Lett.*, vol. 23, pp. 1363–1365, 1998.

[3] W. A. Clarkson and D. C. Hanna, "2-Mirror beam-shaping technique for high-power diode bars," *Opt. Lett.*, vol. 21, no. 6, pp. 375–377, 1996.

[4] M. Pollak, W. F. Wing, R. J. Grasso, E. P. Chicklis, and H. P. Jenssen, "CW laser operation of Nd:YLF," *IEEE J. Quantum Electron.*, vol. QE-18, pp. 159–163, Feb. 1982.

[5] J. E. Murray, "Pulsed gain and thermal lensing of Nd-$LiYF_4$," *IEEE J. Quantum Electron.*, vol. QE-19, pp. 488–491, Apr. 1983.

[6] C. Pfistner, R. Weber, H. P. Weber, S. Merazzi, and R. Gruber, "Thermal beam distortions in end-pumped Nd:YAG, Nd:GSGG and Nd:YLF rods," *IEEE J. Quantum Electron.*, vol. 30, pp. 1605–1615, July 1994.

[7] T. Chuang and H. R. Verdun, "Energy-transfer up-conversion and excited-state absorption of laser-radiation in Nd:YLF laser crystals," *IEEE J. Quantum Electron.*, vol. 32, pp. 79–91, Jan. 1996.

[8] Y. Guyot, H. Manaa, J. Y. Rivoire, R. Moncorgé, N. Garnier, E. Descroix, M. Bon, and P. Laporte, "Excited-state absorption and up-conversion studies of Nd3+ doped single crystals $Y_3Al_5O_{12}$, $YLiF_4$, and $LaMgAl_{11}O_{19}$," *Phys. Rev. B*, vol. 51, no. 2, pp. 784–799, 1995.

[9] A. D. Hays and R. Burnham, "High duty-cycle diode-pumped Nd:YLF slab laser," *Advanced Solid-State Lasers, OSA Tech. Dig. Ser.*, 1993, paper AMD6-1.

[10] T. M. Baer and M. S. Keirstead, "Modeling of End-Pumped, solid-state lasers," *Conference on Lasers and Electro-Optics, OSA Tech. Dig. Ser.*, 1993, pp. 638–640, paper CFM1.

[11] B. Neuenschwander, R. Weber, and H. P. Weber, "Determination of the thermal lens in solid-state lasers with stable cavities," *IEEE J. Quantum Electron.*, vol. 31, pp. 1082–1087, June 1995.

[12] G. Cerullo, S. deSilvestri, and V. Magni, "High-efficiency, 40 W CW Nd:YLF laser with large TEM_{00} mode," *Opt. Commun.*, vol. 93, no. 1–2, pp. 77–81, 1992.

[13] H. Vanherzeele, "Thermal lensing measurement and compensation in a continuous-wave mode-locked Nd:YLF laser," *Opt. Lett.*, vol. 13, no. 5, pp. 369–371, 1988.

[14] K. I. Martin, W. A. Clarkson, and D. C. Hanna, "3-W of single-frequency output at 532 nm by intracavity frequency-doubling of a diode-bar-pumped Nd:YAG ring laser," *Opt. Lett.*, vol. 21, no. 12, pp. 875–877, 1996.

[15] W. A. Clarkson, R. Koch, and D. C. Hanna, "Room-temperature diode-bar-pumped Nd:YAG laser at 946 nm," *Opt. Lett.*, vol. 21, no. 10, pp. 737–739, 1996.

[16] M.E. Innocenzi, H. T. Yura, C. L. Fincher, and R. A. Fields, "Thermal modeling of continuous-wave end-pumped solid-state lasers," *Appl. Phys. Lett.*, vol. 56, no. 19, pp. 1831–1833, 1990.

[17] P. J. Hardman, M. Pollnau, W. A. Clarkson, and D. C. Hanna, "The influence of energy-transfer upconversion on thermal lensing in end-pumped Nd:YLF and Nd:YAG lasers," in *Conf. Lasers and Electro-Optics-Europe, OSA Tech. Dig.*, 1998, p. 151.

[18] W. Koechner, *Solid-State Laser Engineering*, 4th ed. New York: Springer-Verlag, 1996, p. 402.

[19] M. Pollnau, P. J. Hardman, W. A. Clarkson, and D. C. Hanna, "Upconversion, lifetime quenching and ground-state bleaching in Nd^{3+}:$LiYF_4$," *Opt. Commun.*, vol. 147, no. 1–3, pp. 203–211, 1998.

[20] S. Guy, C. L. Bonner, D. P. Shepherd, D. C. Hanna, A. C. Tropper, and B. Ferrand, "High-inversion densities ind Nd:YAG:Upconversion and bleaching," *IEEE J. Quantum Electron.*, vol. 34, pp. 900–909, May 1998.

P. J. Hardman, photograph and biography not available at the time of publication.

W. A. Clarkson, photograph and biography not available at the time of publication.

G. J. Friel, photograph and biography not available at the time of publication.

M. Pollnau, photograph and biography not available at the time of publication.

D. C. Hanna, photograph and biography not available at the time of publication.